AMERICAN SOCIETY FOR MICROBIOLOGY | Journal of Bacteriology

Host-Microbial Interactions | Full-Length Text

Environmental alkalization suppresses deployment of virulence strategies in *Pseudomonas syringae* pv. *tomato* DC3000

Zichu Yang,[1] Haibi Wang,[1] Robert Keebler,[1] Amelia Lovelace,[2] Hsiao-Chun Chen,[3] Brian Kvitko,[3,4] Bryan Swingle[1,5]

AUTHOR AFFILIATIONS See affiliation list on p. 14.

ABSTRACT Plant pathogenic bacteria encounter a drastic increase in apoplastic pH during the early stages of plant immunity. The effects of alkalization on pathogen-host interactions have not been comprehensively characterized. Here, we used a global transcriptomic approach to assess the impact of environmental alkalization on *Pseudomonas syringae* pv. *tomato* DC3000 *in vitro*. In addition to the Type 3 Secretion System, we found expression of genes encoding other virulence factors such as iron uptake and coronatine biosynthesis to be strongly affected by environmental alkalization. We also found that the activity of AlgU, an important regulator of virulence gene expression, was induced at pH 5.5 and suppressed at pH 7.8, which are pH levels that this pathogen would likely experience before and during pattern-triggered immunity, respectively. This pH-dependent control requires the presence of periplasmic proteases, AlgW and MucP, that function as part of the environmental sensing system that activates AlgU in specific conditions. This is the first example of pH-dependency of AlgU activity, suggesting a regulatory pathway model where pH affects the proteolysis-dependent activation of AlgU. These results contribute to deeper understanding of the role apoplastic pH has on host-pathogen interactions.

IMPORTANCE Plant pathogenic bacteria, like *Pseudomonas syringae*, encounter many environmental changes including oxidative stress and alkalization during plant immunity, but the ecological effects of the individual responses are not well understood. In this study, we found that transcription of many previously characterized virulence factors in *P. syringae* pv. *tomato* DC3000 is downregulated by the level of environmental alkalization these bacteria encounter during the early stages of plant immune activation. We also report for the first time the sigma factor AlgU is post-translationally activated by low environmental pH through its natural activation pathway, which partially accounts for the expression Type 3 Secretion System virulence genes at acidic pH. The results of this study demonstrate the importance of extracellular pH on global regulation of virulence-related gene transcription in plant pathogenic bacteria.

KEYWORDS *Pseudomonas syringae*, plant-microbe interactions, environmental sensing, pathogenesis, plant pathology, virulence induction and suppression, transcriptome

Editor Anke Becker, Philipps-Universitat Marburg Fachbereich Biologie, Marburg, Germany

Address correspondence to Bryan Swingle, Bryan.swingle@usda.gov.

The authors declare no conflict of interest.

Received 4 March 2024
Accepted 5 October 2024
Published 24 October 2024

Pathogen-host interactions are naturally antagonistic with both parties employing adaptive strategies to optimize their probability of survival. Plants manage infections using a distributed, non-adaptive immune system in which infections are dealt with locally, with plant cells near the infection site sensing and responding to suppress the growth and spread of pathogens. Several temporally predictable physiological and structural changes mark distinct phases during the infection and immunity process (1, 2). The early stages of infection are critical for determining the outcome of the interaction because the speed of detection and initial efforts to eliminate the pathogens significantly affect the progress of the infection (3). While many of the host responses have been identified (4–11), there is a lack of the understanding of the specific functions of the components as individual factors rather than in combination with the full set of early-stage responses. Understanding the individual effects of early-stage response components would aid optimization of plant immune outputs in disease-resistance breeding programs.

Pseudomonas syringae pv. *tomato* DC3000 (*Pst* DC3000) is a model plant pathogenic bacterium (12). When infecting leaves of host plants, *Pst* DC3000 cells multiply in and deploy their infection strategies from the intercellular space, known as the apoplast (8), near where they enter the leaf tissue. *Pst* DC3000 infection strategies include the production of coronatine to manipulate stomata opening (13), downregulating flagellin synthesis and motility through extracytoplasmic function sigma factor AlgU (14) and reprograming host immunity and physiological response through HrpL-regulated type 3 secretion system (T3SS) and translocated protein effectors (4, 10). In addition, PvdSmediated iron stress responses including siderophore-related functions also contribute to survival under host immunity (3).

On the host side, plants have a two-tiered immune system: PAMP (pathogen-associated molecular patterns)-triggered immunity (PTI) and effector-triggered immunity (ETI). PTI utilizes pattern-recognition receptors on the cell surface to recognize conserved molecular features of microbes such as bacterial flagellin subunits in the apoplast. After kinase-mediated signaling, PTI-triggered cells modify the apoplastic environment and plant cell walls to interfere with infection progress (15). These modifications include increased reactive oxygen species (ROS) burst (5), closure of stomata (9), thickening of cell walls with callose deposition (16), and alkalization of apoplastic fluids (6). Adapted bacterial pathogens attempt to avoid PTI detection and/or suppress PTI responses using the T3SS to inject type 3 secreted effectors (T3Es) into the host cells (2). These effectors (17) or T3E-modified host proteins (18) can stimulate ETI in plants, providing pathogenspecific immunity. During ETI, there is a cascade of events leading to programed cell death and restriction of resources from affected host cells, which work together to limit pathogen growth (1).

Pst DC3000-associated PAMPs can be perceived by the host plant within 1 hour post inoculation (hpi) (13), and T3Es delivery can be detected from about 1.5 hpi (19). The timing of these events suggests that PTI is likely the first system to sense the infection, and PTI-led modifications of the apoplast are the earliest responses to interfere with pathogen growth and virulence. The three earliest PTI-specific modifications of the apoplast are temporally ordered as follows: removal of calcium, alkalization, and then ROS burst (2). The ecological functions of the PTI-generated ROS burst are the best understood among the three. While ROS can be lethal for pathogens without adequate extracellular peroxidase activities, the ROS burst also serves as an intercellular signal for activating transcription of plant immunity genes (20, 21). AlgU activity can be induced by ROS, and the timing of AlgU-dependent expression during *P. syringae* infection correlates with this ROS burst (22, 23). The concentration of calcium estimated in leaf apoplast is sufficient to activate the expression of virulence genes in *Pst* DC3000 through the CvsRS two-component system (24); however, it remains unknown whether the PTI-triggered removal of extracellular calcium can effectively impact disease progression. Alkalization negatively affects fungal colonization (25–27), but its effects during bacterial infection have not been systemically examined. The apoplast of healthy plants prior to PTI (i.e., naïve apoplast) is acidic, with the pH value fluctuating around 5.0 (28–30). Alkalization process starts once PTI is elicited by PAMPs like flagellin or chitin, and the effect can last up to 50–60 hours, raising the apoplastic pH by 0.5–1 unit within the first hour and over 2 units by 24 hours post elicitation (6, 31–33).

Bacterial pathogens, including *Pst* DC3000, respond to environmental pH via various signaling pathways (34–37); however, it remains difficult to infer a complete picture of the

role pH has in pathogen-plant interactions. We, therefore, set out to capture the full transcriptomic landscape of *Pst* DC3000 with environmental pH as the single variable *in vitro*. We hypothesized that alkalization alone can de-activate deployment of *Pst* DC3000 infection strategies, and our data reveal that multiple virulence systems are impacted simultaneously by *in planta*-relevant degrees of alkalization.

RESULTS

Apoplastic pH of mock-treated and PTI-elicited *Arabidopsis thaliana* Col-0 leaves

We first set out to identify the *in planta* pH values relevant to a *Pst* DC3000-host interaction. We induced PTI in *A. thaliana* Col-0 leaves using commercially available flagellin peptides (Flg22) and measured the pH of apoplastic wash fluid (AWF) after 24 hours (38). We estimated the apoplastic pH by multiplying our measurements with either recently published dilution factors (DFs) associated with the AWF preparation protocol or dilution factors determined by tracking dye dilution (30, 39). We found the naïve apoplastic pH to be around 5.54, close to the previously reported leaf apoplastic pH of *A. thaliana* Col-0, while the PTI-elicited leaves have estimated pH over 8.0 (Table 1) (28–30).

Transcriptome analysis of *Pst* DC3000 response to PTI-mimicking alkalization

We used the observed apoplastic pH values to examine the impact of alkalization on the *Pst* DC3000 transcriptome *in vitro*. We exposed log-phase *Pst* DC3000 cultures to three pH levels: 5.5, 6.5, and 7.8, which correspond to the pH of the apoplast before PTI elicitation (naïve), an intermediate level of alkalization, and 24 hours post PTI elicitation, respectively. This was achieved by replacing the King's B (KB) broth of mid-log cultures with pH-adjusted KB media. The exposure lasted 3 hours, over which time we saw slightly more growth at higher pH (Fig. S1). We performed RNA-seq to determine the transcriptomes of these cells and found 423 out of 4,673 total annotated genes to be differentially expressed by strong alkalization (comparing pH 5.5 vs pH 7.8) and about half of the differentially expressed genes (DEGs) also responded to weak alkalization (pH 5.5 vs pH 6.5; Fig. 1A; Table S1). We examined the functional annotations of these DEGs to look for potential ecological implications. We used both Gene Ontology (GO) and Comprehensive Microbial Resource (CMR) annotations for function enrichment analysis and found results from the two annotation databases showed strong agreement (Fig. 1B and C). We found pathogenesis-related functions to be enriched [Fisher's exact test, false discovory rate (FDR) $P < 0.001$] in the set of genes that displayed strong suppression because of alkalization (Fig. 1B and C).

Alkalization affects expression of pathogenesis functions in rich and apoplast mimicking media

More than 75% of the DEGs in the strongly suppressed pathogenesis functional categories (CMR annotation) encode functions related to T3SS or siderophores (Fig. 2A). Even under non-inducing conditions for T3SS (i.e., low baseline expression), the master pathogenicity regulator, *hrpL*, and over half of the known *hrp* regulon, including genes encoding intermediate regulators HrpRS, chaperones, injectosome components, and effectors, were significantly upregulated by low pH and suppressed as a result of alkalization (Fig. 2; Table S1). We confirmed this pattern of regulation for PSPTO_4001

TABLE 1 Measurement of AWF pH and estimation of *A. thaliana* Col-0 apoplastic pH[c]

Treatment	AWF pH measurement (Mean ± SEM, *N* = 6)	Estimate apoplastic pH (dilution factor *F* = 18.25[a])	Estimate apoplastic pH (dilution factor *F* = 2.1466[b])
Mock	6.80 ± 0.04	5.54	6.47
Flg22	7.38 ± 0.07	8.64	7.71

[a]Value calculated using dilution factor by Borniego et al. (30).

pH =is −calculated == as − following: × ⁻ ⁻ =− × ⁻) for acidic AWF pH and [b]Value calculated using dilution factor determined

in this work. Pre-dilution apoplastic (( ))

for basic AWF pH.

[c]Dilution factor .

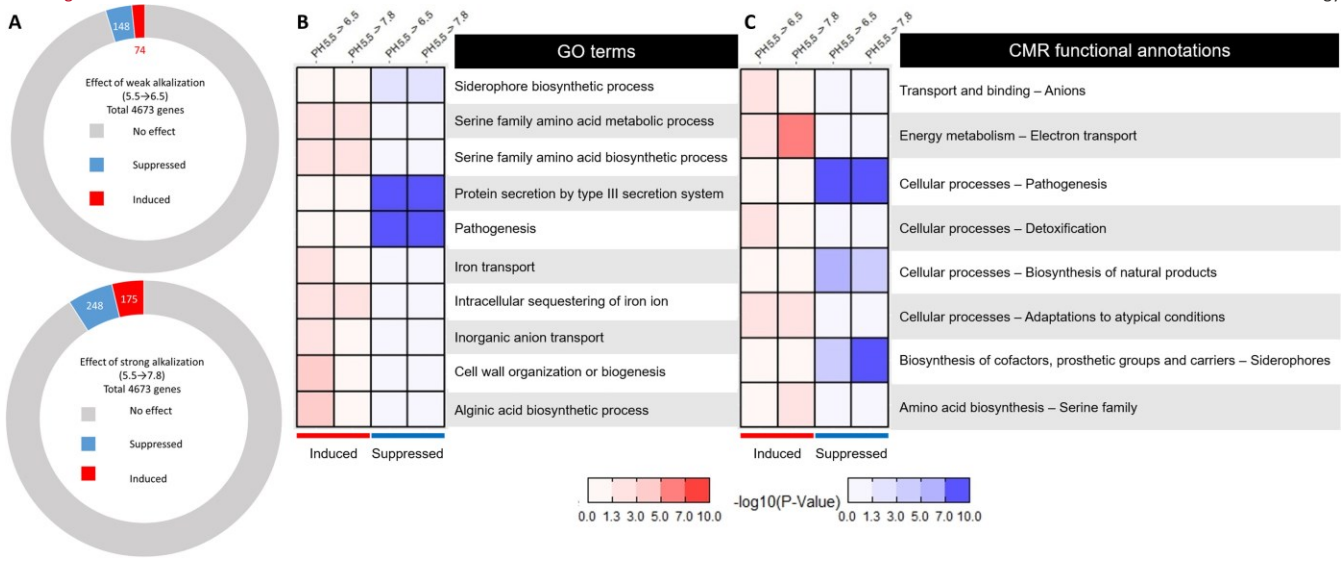

FIG 1 Overview of pH-responsive DEGs in *Pst* DC3000 in modified KB media. (A) pH-responsive DEGs make up less than 10% of the *Pst* DC3000 genome. (B) GO-term enrichment analysis results suggest that alkalization causes a reduction in the expression of virulence-related functions in *Pst* DC3000 (BinGO ver. 3.03; Fisher's exact test, *P*-values adjusted by FDR). (C) Similar results were found with functional category enrichment analysis using CMR functional annotations [downloaded from the J. Craig Venter Institute (JCVI) on or about 8 July 2013]. The complete set of CMR functional annotations for *Pst* DC3000 is available in reference (7). Fisher's exact test, *P*-values adjusted by FDR (7).

(encoding effector AvrPto), which was suppressed 20-fold by alkalization in RNA-seq data and quantitative real-time polymerase chain reaction (qRT-PCR) quantification, as well as PSPTO_0588 (encoding effector HopH1), which was reduced threefold in RNA-seq data and ninefold by qRT-PCR (Fig. 2B). We observed similar trends for both of these genes in apoplast-mimicking hrp-inducing minimal media (HMM), where PSPTO_4001 was 110-fold suppressed by alkalization, and PSPTO_0588 was 15-fold suppressed (Fig. 2B) (40).

Over 50% of TonB-dependent siderophore receptor genes with annotated function in pathogenesis are strongly suppressed in the alkalized conditions (Fig. 2A). In addition to the annotated pathogenesis-related siderophore genes, we found expression of more genes with functions related to iron stress to be strongly (i.e., more than fourfold) suppressed by alkalization, including four iron starvation sigma factors: PSPTO_0444, PSPTO_1203, PSPTO_1286, and PSPTO_2133 (*pvdS*) (41–43). Surprisingly, the expression of PSPTO_4508 (*fur*), the primary iron homeostasis regulator (44) in *Pst* DC3000, was affected less than twofold by pH (Table S1). Iron stress sigma factor, PvdS, helps *Pst* DC3000 survive ETI and is suppressed during leaf infection (3). We found that the expression of 13 out of 16 validated PvdS-regulated genes (41) was suppressed by alkalization, 11 of which were suppressed over fourfold by elevated pH (Table 2; Table S1). Consistent with this, expression of *pvdS* itself was suppressed more than 10-fold in alkalized KB medium (Fig. 2C). However, expression of *pvdS* was induced rather than suppressed in alkalized HMM (Fig. 2C), suggesting nutrient-sensitive co-regulation.

Coronatine was another virulence factor affected by alkalization, but unlike T3SS or iron uptake functions, coronatine synthesis genes (*cfa* genes, *cma* genes, and *cfl*) were suppressed by alkalization to pH 7.8 but appeared to maintain robust expression even at pH 6.5 (Table 3). We used qRT-PCR to confirm that expression of both *cfl* and *cmaE* was suppressed more than 10-fold under strong alkalization in KB-based media (Fig. 2C). However, similar to *pvdS*, both genes were induced by alkalization in HMM (Fig. 2C).

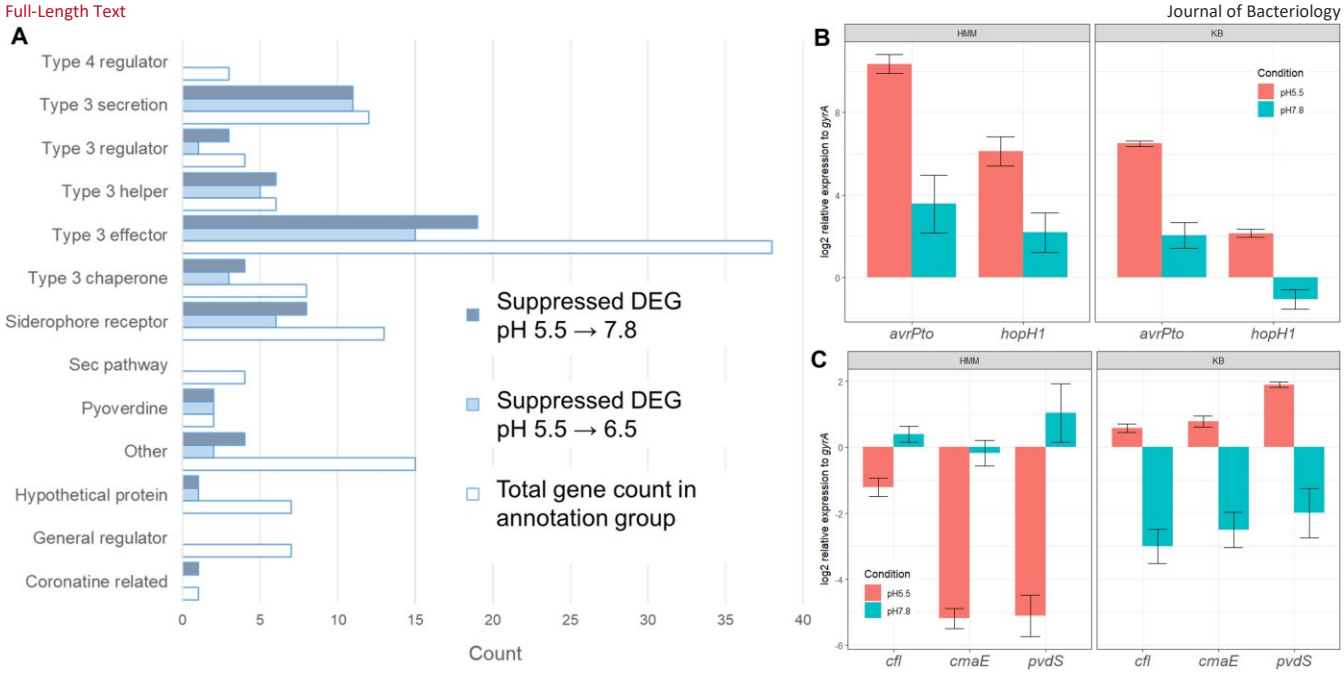

FIG 2 Environmental alkalization strongly suppresses expressions of genes encoding virulence and iron uptake functions. (A) Counts of alkalization-suppressed genes in indicated functional categories. Color-coded responses for weak (5.5 → 6.5) and strong alkalization (5.5 → 7.8). Suppression was determined by both displaying more than twofold change in standardized read numbers and FDR-adjusted *P*-value passing significance threshold of 0.05. (B) qRT-PCR expression fold-change results for representative T3SS genes *avrPto* (PSPTO_4001; student's *t*-test $P < 0.001$, $N = 9$) and *hopH1* (PSPTO_0588; student's *t*-test $P < 0.01$, $N = 9$) in HMM and KB media. Expression of *avrPto* and *hopH1* was 110- and 15-fold higher at pH 5.5 than pH 7.8 in HMM, respectively, and 21- and 9-fold higher in modified KB medium. (C) qRT-PCR expression fold change of representative iron-stress gene *pvdS* (student's *t*-test $P < 0.001$, $N = 9$), coronatine synthesis gene *cmaE* (student's *t*-test $P < 0.01$, $N = 9$), and *cfl* (student's *t*-test $P < 0.001$, $N = 9$) in HMM and KB media. Expression of *cfl*, *cmaE*, and *pvdS* was 3-, 32-, and 71-fold lower at pH 5.5 than pH 7.8 in HMM, respectively. In contrast, *cfl*, *cmaE*, and *pvdS* was 12-, 10-, and 15-fold more expressed at pH 5.5 than pH 7.8 in modified KB medium. All reads were standardized to expression of housekeeping gene *gyrA* (PSPTO_1745). Error bars represent SEM.

AlgU contributes to *Pst* DC3000 pH responses

We examined the pH-dependent transcriptome data for evidence of potential environmental sensing systems that might be capable of transducing information about the external pH into the gene expression responses that we observed. We found that PSPTO_4381 expression, an established reporter of AlgU activity (7), was reduced at elevated pH (Table S1). AlgU is an extracytoplasmic function sigma factor that is

TABLE 2 Expression response of PvdS regulon to alkalization

Locus ID	Description	Log2 fold change (5.5 → 6.5)	Log2 fold change (5.5 → 7.8)
PSPTO_0753	Bcr/CflA family multidrug-resistance transporter	−2.0	−3.2
PSPTO_2134	Pyoverdine synthetase and thioesterase component	−4.1	−4.9
PSPTO_2137	MbtH-like protein	−3.3	−4.8
PSPTO_2146	Pyoverdine biosynthesis regulatory gene	−4.0	−4.9
PSPTO_2147	Pyoverdine sidechain peptide synthetase I, epsilon-Lys module	−3.7	−4.7
PSPTO_2149	Pyoverdine sidechain peptide synthetase III, L-Thr-L-Ser component	−3.9	−4.0
PSPTO_2152	TonB-dependent siderophore receptor	−3.2	−3.7
PSPTO_2156	Renal dipeptidase family protein	−3.4	−4.0
PSPTO_2161	Penicillin amidase family protein	−3.5	−4.1
PSPTO_2175	3-Isopropylmalate dehydrogenase	−0.4	−0.2
PSPTO_2982	Hypothetical protein	−3.0	−2.8
PSPTO_3172	Membrane protein	0.0	−0.1
PSPTO_3290	Outer membrane porin, OprD family	−2.5	−3.2

TABLE 3 Expression responses of known coronatine synthesis genes to alkalization

Locus ID	Description	Log2 fold change (5.5 → 6.5)	Log2 fold change (5.5 → 7.8)
PSPTO_4680	Coronafacic acid synthetase and ligase component Cfl	0.0	−3.0
PSPTO_4681	Coronafacic acid synthetase and acyl carrier protein component	−0.4	−3.1
PSPTO_4682	Coronafacic acid synthetase and dehydratase component	0.0	−2.7
PSPTO_4687	Coronafacic acid polyketide synthetase II	−0.1	−1.2
PSPTO_4689	Crotonyl-CoA reductase	−0.1	−2.5
PSPTO_4707	Coronamic acid synthetase CmaD	0.3	−3.4
PSPTO_4708	Coronamic acid synthetase CmaE	−0.2	−3.3
PSPTO_4711	Coronamic acid synthetase CmaC	−0.1	−2.4
PSPTO_4712	Coronamic acid synthetase and thioesterase component	0.1	−2.3
PSPTO_4714	CmaU protein	0.1	−1.3

activated *in planta* and has an important role in activating virulence gene expression in the early stages of infection (7, 14, 45). Activation of AlgU in response to environmental conditions involves several proteases that sequentially cleave MucA, the membrane-bound anti-sigma factor controlling AlgU activity. This process of regulated intermembrane proteolysis (RIP) relies on the function of AlgW and MucP to sense stimulatory environmental cues and post-translationally de-inhibit AlgU (45, 46). We compared our pH-dependent transcriptome results with the AlgU regulon (7) and found that 126 AlgU-regulon members were also differentially expressed. In this set of pH-responsive AlgU-regulated genes, 67 were downregulated by alkalization and included the majority of virulence-related genes (Fig. 3A; Table S1). However, we also found that 59 of pH-responsive AlgU-regulated genes were upregulated by alkalization, including those for alginate production and NADH-related functions. This suggested that the pH-responsive AlgU-regulated genes are possibly controlled by other regulators in addition to AlgU. It is worth noting that expression of *algW* (PSPTO_4435) was affected by environmental pH in HMM similarly to PSPTO_4381, showing high expression at pH 5.5 and reduced expression at pH 7.8 (Fig. 3B; Table S1), while the expression of *mucP* (PSPTO_1541) did not appear altered between the two pH levels. We also found that the expression of *algU* (PSPTO_4224) and *mucA* (PSPTO_4223) was increased at pH 7.8 (Table S1); however, this is unlikely to have significant effects because AlgU-dependent expression is primarily controlled by post-translational regulation of AlgU activity (7).

We attempted to address the question of whether acidic pH is capable of stimulating AlgU activity by focusing on expression of PSPTO_4381. The PSPTO_4381 gene was chosen because its expression previously showed a complete dependence on AlgU, and we found no evidence that it is affected by other regulators (7). In contrast, other AlgU-regulated genes like *algD* show complex expression patterns that involve other regulators (47–50). We used qRT-PCR and a P$_{PSPTO_4381}$:: *lux* promoter fusion to test AlgU activity in wild-type and *algU*-deleted *Pst* DC3000 strains after 3-hour incubation in KB at 5 pH levels, ranging from pH 5.4 to 7.0 (Fig. 3B and C) (7). We found that AlgU-dependent *lux* expression was highest at pH 5.4 (Fig. 3C) and was reduced by twofold as pH increases from 5.4 to 7.8 (Fig. 3C). This pattern of expression was confirmed using qRT-PCR to monitor PSPTO_4381 expression from its native location (Fig. 3B).

AlgU activity is controlled post-translationally by a membrane bound anti-sigma factor (MucA) and conditionally activated proteases (i.e., AlgW and MucP*)* located in the periplasm. These proteases are activated by membrane stress and ensuing misfolded proteins in the periplasm to cleave the MucA anti-sigma factor and eliminate its ability to inhibit AlgU activity. We tested whether components of this RIP cascade were necessary for pH-stimulated AlgU activity by comparing P$_{PSPTO_4381}$:: *lux* reporter activity in wild-type, *algU*, and *algW mucP* deletion strains. We found that reporter expression in the *algW mucP* double deletion strain was indistinguishable from the *algU* deletion mutant (Fig. 3C), indicating that the activation of AlgU by acidic pH requires a function

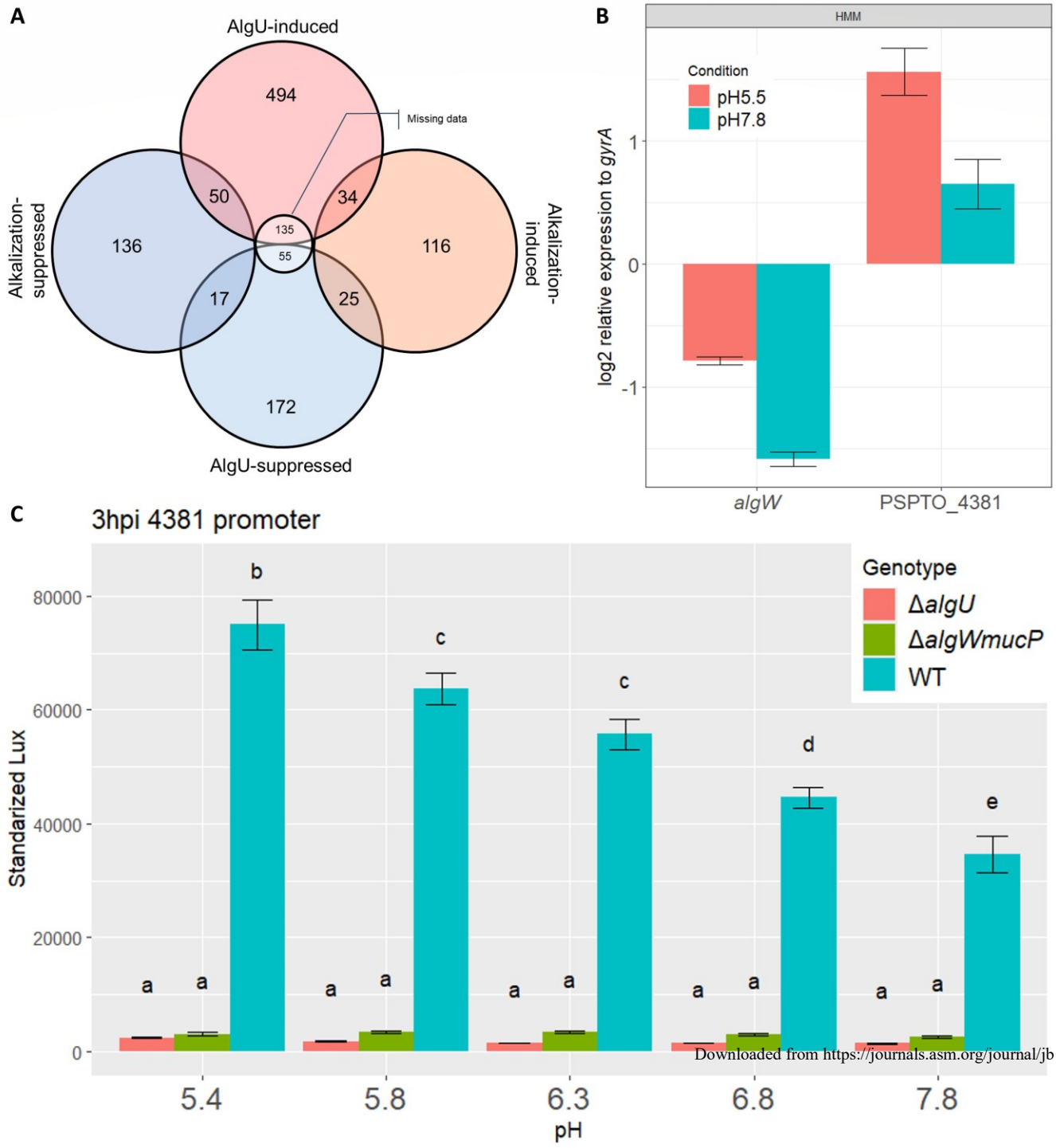

FIG 3 AlgU activity is sensitive to pH *in vitro*. (A) Graphic summary of intersections between alkalization stimulon and previously identified AlgU-regulon. Genes from the AlgU regulon that did not have normalized counts after trimming and quality check from the analysis pipeline were labeled as missing data. (B) qRT-PCR results of effects of alkalization on *algW* and PSPTO_4381 expression in HMM. Expression of *algW* and PSPTO_4381 was 1.9- and 1.75-fold higher at pH 5.5 than pH 7.8, respectively. Error bars represent SE. (C) Activity of PSPTO_4381 promoter is suppressed by alkalization in modified KB media, and this suppression is dependent on the presence of AlgU as well as its natural proteolysis activation pathway. Standardized Lux activity was calculated as the luminescence/OD_{600} after 3-hour incubation (see Materials and Methods). Error bars represent SEM, and group letters were assigned by Tukey post-hoc test ($N = 9$).

of these RIP sensory components. These results indicate that AlgU activity is affected by environmental pH and likely through the natural RIP pathway.

AlgU has a massive regulon spanning 20% of *Pst* DC3000 genome, many of these genes are also controlled by additional regulators that serve to adjust the extent of the regulon expressed to meet the needs of specific conditions (7, 24, 50–55). To identify the set of genes that require AlgU to respond to alkalization, we used RNA-seq to compare the transcriptomes of wild-type *Pst* DC3000 and an *algU* deletion mutant at pH 5.5 and 7.8. The *algU* deletion mutant showed similar growth patterns to that of wild type in pH-adjusted KB media (Fig. S1). We found 155 DEGs that require AlgU for differential expression between pH 5.5 and pH 7.8. This set was enriched for genes encoding functions related to pathogenesis, siderophore biosynthesis and uptake, and electron transport-related genes (Fig. 4; Fisher's exact text, FDR-adjusted $P < 0.001$ for each functional category). Many pathogenesis and siderophore genes showed complete or partial reduction in their response to pH in the absence of AlgU (Fig. 4A; Table S1). We confirmed that the expression of representative T3SS genes also required AlgU for pH-dependent regulation in apoplastic-mimicking HMM. Expression of *avrPto*, *hrpL*, and *hopH1* was 110-, 35-, and 15-fold higher in HMM at pH 5.5 than pH 7.8, with AlgU accounting for 95-, 32-, and 15-fold difference in expression between the two pHs, respectively (Fig. 4B). These results are consistent with the hypothesis that AlgU activity in response to environmental pH contributes to the transcriptomic difference of *Pst* DC3000 between pH 5.5 and pH 7.8.

DISCUSSION

In this study, we conducted a series of RNA-seq experiments to characterize *Pst* DC3000 responses to strong alkalization *in vitro* and to identify that the AlgU extracytoplasmic sensing system contributes to pH-responsive gene regulation. Our results show that even in rich media conditions, which are not typically thought to be favorable for inducing virulence gene expression, many pathogenesis genes show detectable differences in expression between low- and high-pH environments. We confirmed that T3SS and T3E genes were similarly regulated in pH-adjusted HMM, which was designed to mimic conditions bacteria experience in plant apoplast during infections. Coronatine synthesis and iron stress responses are impacted by alkalization, but the relationship is more intricate. Specifically, the nutrient condition of the media influences whether alkalization leads to increased or decreased expression. These results suggest that environmental pH is an important cue affecting all major virulence systems of *Pst* DC3000.

We found that pH-dependent expression of two representative T3SS genes (*avrPto* and *hrpL*) was regulated by AlgU, and alkalized conditions do not support AlgU-dependent expression of these functions. We found that AlgU activity is induced at low pH, and this occurs through the native extracytoplasmic sensing system that controls AlgU activity by intermembrane proteolysis (Fig. 3). Expression of major AlgU-regulated virulence genes is induced at pH 5.5, which is equivalent to the conditions bacteria experience when they enter naïve apoplast. These same virulence systems are downregulated at pH 7.8, which is equivalent to the pH of immune-activated conditions that occur during PTI. We hypothesize that alkalization of plant apoplast during PTI is an adaptation to prevent systems regulated by AlgU (particularly those involved with virulence) from being expressed properly and could explain how PTI-activated plants become immune to normally virulent *Pst* DC3000 and block translocation of *Pst* DC3000 T3Es (3, 56, 57). We attempted to test this idea by modifying apoplastic pH of *A. thaliana* Col-0 leaves with MOPS and MES buffer immediately after infecting with wild-type *Pst* DC3000. However, the results were inconclusive because we were not able to maintain the pH modification throughout the time needed to span from inoculation through symptom appearance (data not shown).

Our results show that many genes, especially those encoding functions related to pathogenesis, are dependent on AlgU to be expressed in response to low pH. However, only a portion of the previously identified AlgU regulon was found to be controlled by pH (Fig. 3A). This might be attributable to differences between induction of AlgU

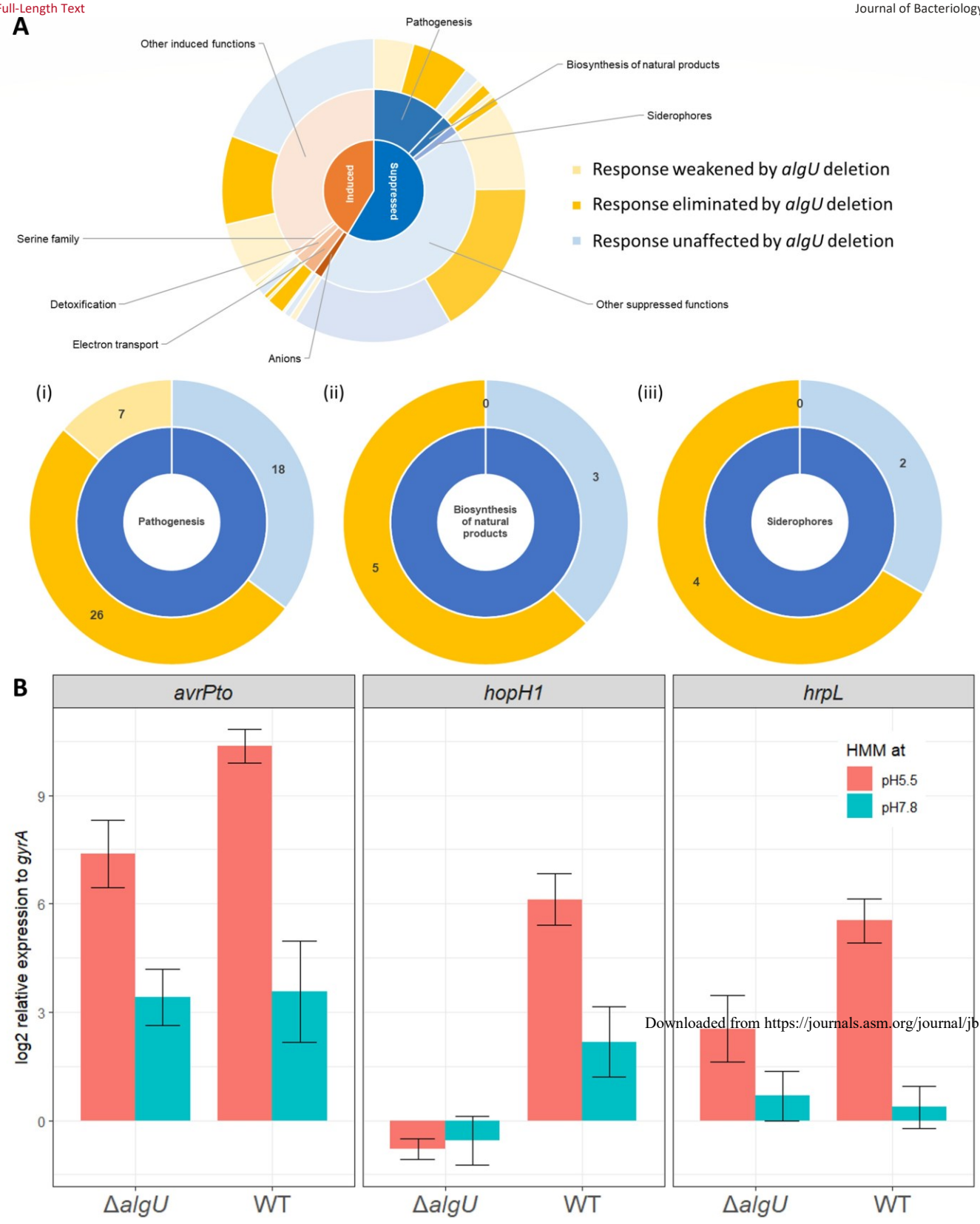

FIG 4 AlgU contributes to pH-dependent transcriptomic changes. (A) Overview of *Pst* DC3000 alkalization-induced (5.5 → 7.8) transcriptomic responses and effects of *algU* deletion on each of the major alkalization-affected functional categories. Response was considered weakened when the change in DEG expression was reduced from at least fourfold in wild type to not less than twofold in the *algU* deletion strain. (i), (ii), and (iii) Number of genes dysregulated

(Continued on next page)

Fig 4 (Continued)

by *algU* deletion in the three major alkalization-suppressed functional categories. Genes and detailed fold-change data are listed in Table S2. (B) Effects of alkalization and *algU* deletion on expression of representative T3SS genes in HMM at 3 hpi. Error bars represent SEM. Deletion of *algU* resulted in reduced expression of all three genes (*avrPto*, *hopH1*, and *hrpL*) at pH 5.5, but *hopH1* was also affected at pH 7.8. Expression of *avrPto*, *hrpL*, and *hopH1* was 110-, 35-, and 15-fold higher in HMM at pH 5.5 than pH 7.8, with AlgU accounting for 95-, 32-, and 15-fold difference in expression between the two pHs, respectively.

activity through its natural extracytoplasmic sensing system compared to overexpression of AlgU in a *mucAB* deletion background as was used to define the AlgU-regulon. Alternatively, additional regulators may modulate AlgU-dependent expression (50) to limit expression to only the functions needed for specific conditions (Table S1). For example, the effect of alkalization on T3SS gene expression is greater in HMM and *in planta* (58) compared to what we observed in KB. Furthermore, only a subset of the complete AlgU regulon shows AlgU-dependent expression in *Pst* DC3000 exposed to naïve and PTI-elicited plants (59) (Table S2).

Transcription of *algU* (PSPTO_4224) and *mucA* (PSPTO_4223) was significantly upregulated at higher pH levels, which appear contradictory to our hypothesis that AlgU activity is suppressed at elevated pH. However, regulation of *algU* gene expression is not the predominate mechanism controlling expression of AlgU-regulated gene in *Pst* DC3000. Our previous work showed that expression of AlgU-regulated genes is undetectable in non-inducing conditions even with *algU* overexpression, and *mucAB* must be deleted to detect AlgU-dependent gene expression in non-inducing condition (7). Therefore, our result suggests that the acidic environments, as found in naïve apoplast, stimulate post-translational activation of AlgU, adding to the set of environmental conditions known to activate *P. syringae* AlgU (22, 45, 60). We also note that no evidence of activation was found when *P. aeruginosa* AlgU was tested for activation by HCl (61).

AlgW and MucP are both proteases in the proteolysis pathway that carries out the natural de-inhibition of AlgU (45, 62, 63). We do not yet know how AlgW or MucP are involved in activating AlgU in response to low pH conditions. Environmental pH can potentially affect the abundance of misplaced outer membrane proteins and lipopolysaccharide in the periplasm, which are detected by AlgW through protein binding
(64). We found that the *algW* gene was expressed at higher level at pH 5.5 than 7.8, which could potentially increase the pH sensitivity by altering the abundance of AlgW proteins available to trigger AlgU activation. Acid shock activates σ^E, the AlgU homolog in *Salmonella enterica*, but this only requires DegP, the MucP homolog (65). However, unlike *algW, mucP* expression was not altered between two environmental pHs in our RNA-seq results. In these experiments, we used the *algW*/*mucP* deletion mutant, which was useful to test whether this environmental sensing system was involved in pH-dependent activation of AlgU. However, we cannot conclude if either or both AlgW and MucP are needed for acidic activation of AlgU in *Pst* DC3000.

It is necessary to use an acidic pH medium to detect *P. syringae* T3SS activity *in vitro*, which mimics the virulence-inducing environment of the apoplast (4, 66, 67). Our results are consistent with the notion that T3SS transcription is minimal at neutral to alkalized pH, and acidification alone is sufficient to induce T3SS expression regardless of nutrient composition of the media. Acidic pH is also an important cue for inducing T3SS expression in other bacterial pathogens via various mechanisms. In human pathogenic *Shigella sp.*, environmental pH is monitored by CpxAR, a two-component system that can de-inhibit expression of transcriptional regulator, *VirF* (68, 69). Environmental pH affects *Shigella* T3SS activity through modification of functional protein complexes such as T3SS injectisome (70). Similarly, in *S. enterica*, environmental pH affects T3SS post-transcriptionally, through translation regulation, protein oligomerization, and protein-complex formation (71, 72).

Iron starvation is a vital component of host-pathogen interactions as well as microbial competition (73, 74). Interfering with iron uptake by suppressing the expression of the PvdS-regulated iron uptake system under conditions where iron is scarce may help limit bacterial growth for the host. Similar strategies are a part of host defense mechanisms in other host-pathogen interactions such as heme in animal intestinal infections (74–76). Our data show that in a rich medium, alkalization can significantly suppress expression of genes related to iron stress response, and the opposite occurs in HMM. This reversal of expression patterns

on *pvdS* suggests that in addition to environmental pH, iron stress genes (and similarly coronatine biosynthesis genes) are likely co-regulated in response to abundance of environmental nutrients.

Finding that alkalization eliminated AlgU activity and *hrp* gene expression poses an interesting question: is the pH of naïve apoplast one of the major cues to activate virulence upon *P. syringae* entry into the host? While we do not yet know the magnitude of the pH change bacteria experience when moving from plant surfaces into the apoplast, previous studies in *Pst* DC3000 T3SS have shown that apoplast-mimicking environments contain cues such as pH, metabolites, and temperature that can activate virulence gene expression (4, 34, 77). Our data further suggest that major *Pst* DC3000 virulence systems appear most transcriptionally active when environmental pH is closer to the naïve apoplastic pH than PTI-induced conditions of the plant host. This is consistent with the observation that small organic acids from the plant host can help induce T3SS in *Pst* DC3000 (77). Evolutionarily, tuning the AlgU extracytoplasmic sensing system to have maximal activity at near-naïve apoplastic pH seems to support the goal of host-evasion as it would allow AlgU-mediated downregulation of flagellar biosynthesis and upregulation of virulence genes to begin immediately after *Pst* DC3000 enters the host apoplast. It is likely worthwhile to investigate in the future how the periplasmic sensory system detects environmental pH in *Pst* DC3000, and whether maintaining high environmental pH can be used for bacterial disease management.

MATERIALS AND METHODS

Bacteria strains and growth conditions

Pst DC3000 strains (Table 4) were grown at 28°C in KB medium (78) and on KB medium solidified with 1.5% (wt/vol) agar. *Escherichia coli* TOP10 (Invitrogen) strains were grown at 37°C in LB medium and on LB medium solidified with 1.5% (wt/vol) agar (79). Kanamycin was supplied at 50 µg/mL, and gentamycin was supplied at 10 µg/mL. Plasmid DNAs were isolated using Qiagen Miniprep Kit (Qiagen) from overnight cultured *E. coli* TOP10 cells and subsequently used to transform *Pst* DC3000 and mutant derivatives by electroporation (80).

pH altered KB medium was prepared according to the standard recipe (78) except for the addition 11% (vol/vol) of 1 M potassium phosphate buffer for a final concentration of 0.11 M phosphate buffer. One molar potassium phosphate buffer at pH 5.4, 5.5, 5.8, 6.3, 6.5, 6.8, and 7.8 was prepared by adjusting the ratios of the mono- and dibasic potassium phosphate solutions, so all buffers had the same osmolarity. pH-altered HMM was prepared similarly by making the standard recipe media (40) without phosphate buffer and later adding in 11% (vol/vol) 1 M potassium phosphate buffer to achieve final concentration of 0.11 M phosphate buffer.

TABLE 4 Strains and plasmids used

Strain or plasmid	Relevant characteristic(s)	Reference
Strains		
PS1	*P. syringae* pv. *tomato* DC3000 wild type	(12)
PS554	*P. syringae* pv. *tomato* DC3000 Δ*algU*	(7)
PS1382	*P. syringae* pv. *tomato* DC3000 Δ*algW* Δ*mucP*	This work
Plasmids		
pEM63	P_{PSPTO_4381}::*lux* Km_r	(7)
pEM64	P_{PSPTO_1417}::*lux* Km_r	(7)
pEM65	P_{algD}::*lux* Km_r	(7)
pEM66	P_{PSPTO_1185}::*lux* Km_r	(7)
pDONR1K18ms		(81)

Extraction of apoplastic wash fluid

AWF was extracted using vacuum infiltration as described by O'Leary et al. with slight modifications (39). Leaves from 4.5-week-old *A. thaliana* Col-0 were treated with either 1 µM Flg22 elicitor (GenScript) in 0.1% dimethyl sulfoxide to induce PTI or the 0.1% dimethyl sulfoxide mock buffer as control via blunt-end syringe infiltration. Leaf samples were collected at 20-hour post-treatment and submerged in cold distilled water. Repeated cycles of vacuum at 95 kPa on ice for 2 min followed by slow release of pressure were applied until leaves were fully infiltrated. Excess water was blotted from plant tissue before leaves were rolled into Saran wrap which were placed into 50 mL conical tubes. Tubes were centrifuged at 1,000 rpm for 10 min at 4°C, and the fractions were pooled and centrifuged at 16,000 × g for 10 min at 4°C to separate the supernatant from insoluble debris. DF of the extracted AWF was estimated using indigo carmine infiltration in parallel. Briefly, the dilution factor was calculated by the $OD_{610infiltrate}$/ ($OD_{610infiltrate}$ − OD_{610AWF}) as described by O'Leary et al. (39).

Pst DC3000 *algW mucP* double mutant construction

We used standard marker exchange mutagenesis to sequentially produce a *Pst* DC3000 strain with both the *algW* (PSPTO_4435) and *mucP* (PSPTO_1541) genes deleted (82). Deletion constructs for each gene were made using synthetic linear DNA fragments from Twist Bioscience that contained ~500 bp flanking each gene joined together with an XmaI (cccggg) site and *attB* sites added to the 5' and 3' ends (Table S3). The DNA fragments were incorporated into pDONR1K18ms (81) by Gateway cloning (Thermo Fisher Scientific). The plasmid carrying the *algW* deletion construct was transformed into wild-type *Pst* DC3000 strain, and merodiploids were selected for kanamycin resistance. Sucrose counter selection was used to select for recombinants that had subsequently eliminated the deletion construct plasmid backbone and confirmed to be sensitive to kanamycin. We confirmed deletions by sequencing PCR products amplified with primers that annealed to sequences flanking the deleted *algW* locus. This process was repeated using the *algW* deletion strain to introduce the *mucP* deletion.

In vitro bacteria culture for RNA-seq and growth curve measurement

Both wild type and Δ*algU* mutant of *Pst* DC3000 strains were grown overnight in standard KB and then resuspended in 5 mL of pH-altered KB media at OD_{600} value of 0.4 from NanoDrop oneC (Theromo Fisher). We set aside 1 mL from each of these cultures to record their growth curves. The remaining cultures were incubated for 3 hours at 28°C with shaking and subsequently collected for RNA extraction. For each combination of strain and media pH, we allocated 200 µL of that culture per well in triplicate into a 96-well plate and monitored OD_{600} values over a 3-hour incubation period at 28°C with shaking with a Synergy 2 plate reader (BioTek).

RNA extraction and quality control

Pst DC3000 cultures were pelleted by centrifugation and resuspended in TriZol reagent (Invitrogen). RNA was subsequently extracted from each sample using the Direct-Zol RNA MiniPrep kit (Zymo Research, Irvine, CA) following the manufacturer's instructions. An additional DNAse treatment was performed with Ambion DNase I (Invitrogen) before final elution. Three samples were collected for each combination of strain and media pH. RNA sample quality was confirmed using a Qubit (RNA HS kit; Thermo Fisher) to determine concentration and with a Fragment Analyzer (Agilent) to determine RNA integrity at Cornell Biotechnology Resource Center.

RNA-seq library preparation and sequencing and analysis

Total RNA samples were treated with a NEBNext rRNA depletion kit (NEB) to remove rRNA. Unique dual indexes (UDI)-barcoded RNAseq libraries were generated with the NEBNext Ultra II RNA Library Prep Kit (NEB). Each library was quantified with a Qubit (dsDNA HS kit; Thermo Fisher), and the size distribution was determined with a Fragment Analyzer (Agilent)

prior to pooling. Libraries were then sequenced on an Illumina instrument, and we generated 10 M reads per library.

RNA-seq analysis

Low-quality and adaptor sequences were trimmed with TrimGalore (v0.6.0), a wrapper for cutadpt and fastQC, with the parameters as following: -j 1 -e 0.1 –nextseq-trim = 20 -O 1 -a AGATCGGAAGAGC –length 50 –fastqc. Remaining reads were mapped to reference genome (12) with STAR (v2.7.0e). Normalized counts of reads and following statistical analysis of differential gene expression were then carried out with SARTools and DESeq2 (v1.26.0). Subsequent analyses and plotting were performed in R (4.3.2) using package ggplot2 (v.3.4.2), ggbreak (v.0.1.2), and tidyr (v.1.3.0). We used the conservative cut-off threshold and considered only genes with adjusted *P*-value of <0.05 and more than twofold expression change as differentially expressed genes.

Quantitative real-time PCR

We carried out reverse transcription with RNA prepared for transcriptome analysis using iScript cDNA synthesis kit (Bio-Rad, Hercules, CA). The cDNA product was diluted 10-fold with water, and we used 1 µL per technical replicate for quantitative PCR analysis. The qRT-PCR was run with Bio-Rad CFX Connect real-time PCR detection system in combination with SsoAdvanced universal SYBR green (Bio-Rad) following manufacturer-provided instructions. Cycling protocol was set as follows: 95°C for 3 minutes for initial denaturing, then 40 cycles of 15 seconds at 95°C, 30 seconds at 52°C, and 30 seconds at 60°C. Housekeeping gene *gyrA* was used for baseline standardization (83, 84). All primer sequences of *Pst* DC3000 genes are listed in Table S3.

Lux reporter assay and analysis

Pst DC3000 strains harboring reporter plasmids were recovered from glycerol stocks stored at −80°C by streaking and growing overnight at 28°C on KB agar plates. Cells from these plates were used to inoculate liquid KB and grown overnight at 28°C with shaking. Overnight cultures were washed with fresh KB media and resuspended in pH-altered KB media and adjusted to an OD_{600} of 0.6. For each reporter strain, 200 µL of adjusted culture was loaded to each of three replicate wells on 96-well plates. Two hundred microliter of each pH-adjusted KB medium was loaded in triplicate as sterile media controls. The luminescence (Lux) and OD_{600} were monitored at 10 minutes interval for each well throughout 7.5 hours of incubation at 28°C using a BioTek2 plate reader. The whole process was repeated three times.

For each non-control well within the same biological replicates, standardized Lux signal was calculated with the following formula (Control lux and control OD_{600} reads are taken from sterile media).

$$\mathrm{StdLux} = \frac{\mathrm{ODLux} - \mathrm{CtrlLuxMean}}{\mathrm{CtrlOD\ Mean}}$$

All nine reads of standardized Lux for each strain and pH were then pooled for subsequent ANOVA and Tukey post-hoc analysis in R (v.4.3.2).

ACKNOWLEDGMENTS

We thank Adam Bogdanove, Melanie Filiatrault, Stephen C. Winans, Wei Zhang, Lingwei Wan, and Mary Ann Karp for many helpful discussions. We thank Jen Grenier, Ann E. Tate, and other members of Cornell Transcriptional Regulation and Expression (TREx) facility for their discussions and technology support with RNAseq.

Mention of trade names or commercial products in this publication is solely for the purpose of providing specific information and does not imply recommendation or endorsement by the United States Department of Agriculture. USDA is an equal opportunity provider and employer.

AUTHOR AFFILIATIONS

[1]Plant Pathology and Plant-Microbe Biology Section, School of Integrative Plant Science, Cornell University, Ithaca, New York, USA
[2]The Sainsbury Laboratory, Norwich Research Park, Norwich, United Kingdom
[3]Department of Plant Pathology, University of Georgia, Athens, Georgia, USA
[4]The Plant Center, University of Georgia, Athens, Georgia, USA
[5]United States Department of Agriculture-Agricultural Research Service, Emerging Pests and Pathogens Research Unit, Robert W. Holley Center, Ithaca, New York, USA

AUTHOR ORCIDs

Amelia Lovelace http://orcid.org/0000-0002-6793-7493
Brian Kvitko http://orcid.org/0000-0002-9094-4069
Bryan Swingle http://orcid.org/0000-0001-5048-7791

AUTHOR CONTRIBUTIONS

Zichu Yang, Conceptualization, Data curation, Formal analysis, Investigation, Methodology, Validation, Writing – original draft, Writing – review and editing | Haibi Wang, Investigation, Methodology, Writing – review and editing | Robert Keebler, Investigation | Amelia Lovelace, Methodology | Hsiao-Chun Chen, Investigation, Methodology | Brian Kvitko, Conceptualization, Funding acquisition, Investigation, Methodology, Project administration, Resources, Supervision, Validation, Writing – review and editing | Bryan Swingle, Conceptualization, Funding acquisition, Investigation, Methodology, Project administration, Resources, Supervision, Writing – review and editing

DATA AVAILABILITY

Sequencing data for all RNA-seq experiments are accessible at GSE277531 in the Gene Expression Omnibus (GEO) database.

ADDITIONAL FILES

The following material is available online.

Supplemental Material

Figure S1 (JB00086-24-s0001.docx). Growth of wild-type Pst DC3000 and algU deletion mutant in pH-adjusted KB media.
Table S1 (JB00086-24-s0002.xlsx). RNAseq results and comparison with AlgU regulon.
Table S2 (JB00086-24-s0003.xlsx). AlgU-dependent pH-responsive genes.
Table S3 (JB00086-24-s0004.xlsx). Primers used.

REFERENCES

1. Jones JDG, Dangl JL. 2006. The plant immune system. Nat New Biol 444:323–329. https://doi.org/10.1038/nature05286
2. Yu X, Feng B, He P, Shan L. 2017. From chaos to harmony: responses and signaling upon microbial pattern recognition. Annu Rev Phytopathol 55:109–137. https://doi.org/10.1146/annurev-phyto-080516-035649
3. Nobori T, Velásquez AC, Wu J, Kvitko BH, Kremer JM, Wang Y, He SY, Tsuda K. 2018. Transcriptome landscape of a bacterial pathogen under plant immunity. Proc Natl Acad Sci U S A 115:E3055–E3064. https://doi.org/10.1073/pnas.1800529115
4. Collmer A, Badel JL, Charkowski AO, Deng WL, Fouts DE, Ramos AR, Rehm AH, Anderson DM, Schneewind O, van Dijk K, Alfano JR. 2000. *Pseudomonas syringae* Hrp type III secretion system and effector proteins. Proc Natl Acad Sci U S A 97:8770–8777. https://doi.org/10.1073/pnas.97.16.8770
5. Torres MA, Jones JDG, Dangl JL. 2006. Reactive oxygen species signaling in response to pathogens. Plant Physiol 141:373–378. https://doi.org/10.1104/pp.106.079467
6. Jeworutzki E, Roelfsema MRG, Anschütz U, Krol E, Elzenga JTM, Felix G, Boller T, Hedrich R, Becker D. 2010. Early signaling through the Arabidopsis pattern recognition receptors FLS2 and EFR involves Ca^{2+}-associated opening of plasma membrane anion channels. Pl J 62:367–378. https://doi.org/10.1111/j.1365-313X.2010.04155.x
7. Markel E, Stodghill P, Bao Z, Myers CR, Swingle B. 2016. AlgU controls expression of virulence genes in *Pseudomonas syringae* pv. *tomato* DC3000. J Bacteriol 198:2330–2344. https://doi.org/10.1128/JB.00276-16
8. Couto D, Zipfel C. 2016. Regulation of pattern recognition receptor signalling in plants. Nat Rev Immunol 16:537–552. https://doi.org/10.1038/nri.2016.77
9. Melotto M, Zhang L, Oblessuc PR, He SY. 2017. Stomatal defense a decade later. Plant Physiol 174:561–571. https://doi.org/10.1104/pp.16.01853
10. Xin X-F, Kvitko B, He SY. 2018. *Pseudomonas syringae*: what it takes to be a pathogen. Nat Rev Microbiol 16:316–328. https://doi.org/10.1038/nrmicro.2018.17
11. Ishiga T, Ishiga Y, Betsuyaku S, Nomura N. 2018. AlgU contributes to the virulence of *Pseudomonas syringae* pv. tomato DC3000 by regulating production of the phytotoxin coronatine. J Gen Plant Pathol 84:189–201. https://doi.org/10.1007/s10327-018-0775-6
12. Buell CR, Joardar V, Lindeberg M, Selengut J, Paulsen IT, Gwinn ML, Dodson RJ, Deboy RT, Durkin AS, Kolonay JF, et al. 2003. The complete genome

sequence of the Arabidopsis and tomato pathogen *Pseudomonas syringae* pv. *tomato* DC3000. Proc Natl Acad Sci U S A 100:10181–10186. https://doi.org/10.1073/pnas.1731982100
13. Melotto M, Underwood W, Koczan J, Nomura K, He SY. 2006. Plant stomata function in innate immunity against bacterial invasion. Cell 126:969–980. https://doi.org/10.1016/j.cell.2006.06.054
14. Bao Z, Wei H-L, Ma X, Swingle B. 2020. *Pseudomonas syringae* AlgU downregulates flagellin gene expression, helping evade plant immunity. J Bacteriol 202:e00418-19. https://doi.org/10.1128/JB.00418-19
15. Zipfel C. 2014. Plant pattern-recognition receptors. Trends Immunol 35:345–351. https://doi.org/10.1016/j.it.2014.05.004
16. Luna E, Pastor V, Robert J, Flors V, Mauch-Mani B, Ton J. 2011. Callose deposition: a multifaceted plant defense response. Mol Plant Microbe Interact 24:183–193. https://doi.org/10.1094/MPMI-07-10-0149
17. Dodds PN, Lawrence GJ, Catanzariti A-M, Teh T, Wang C-IA, Ayliffe MA, Kobe B, Ellis JG. 2006. Direct protein interaction underlies gene-for-gene specificity and coevolution of the flax resistance genes and flax rust avirulence genes. Proc Natl Acad Sci U S A 103:8888–8893. https://doi.org/10.1073/pnas.0602577103
18. Eulgem T. 2005. Regulation of the Arabidopsis defense transcriptome. Trends Plant Sci 10:71–78. https://doi.org/10.1016/j.tplants.2004.12.006
19. Grant MR, Kazan K, Manners JM. 2013. Exploiting pathogens' tricks of the trade for engineering of plant disease resistance: challenges and opportunities. Microb Biotechnol 6:212–222. https://doi.org/10.1111/1751-7915.12017
20. Chi M-H, Park S-Y, Kim S, Lee Y-H. 2009. A novel pathogenicity gene is required in the rice blast fungus to suppress the basal defenses of the host. PLoS Pathog 5:e1000401. https://doi.org/10.1371/journal.ppat. 1000401
21. Jwa N-S, Hwang BK. 2017. Convergent evolution of pathogen effectors toward reactive oxygen species signaling networks in plants. Front Plant Sci 8:1687. https://doi.org/10.3389/fpls.2017.01687
22. Keith LMW, Bender CL. 1999. AlgT (ç22) controls alginate production and tolerance to environmental stress in *Pseudomonas syringae*. J Bacteriol 181:7176–7184. https://doi.org/10.1128/JB.181.23.7176-7184.1999 23. Keith RC, Keith LMW, Hernández-Guzmán G, Uppalapati SR, Bender CL. 2003. Alginate gene expression by *Pseudomonas syringae* pv. *tomato* DC3000 in host and non-host plants. Microbiology (Reading, Engl) 149:1127–1138. https://doi.org/10.1099/mic.0.26109-0
24. Fishman MR, Zhang J, Bronstein PA, Stodghill P, Filiatrault MJ. 2018. Ca^{2+}induced two-component system CvsSR regulates the type III secretion system and the extracytoplasmic function sigma factor AlgU in *Pseudomonas syringae* pv. *tomato* DC3000. J Bacteriol 200:e00538-17. https://doi.org/10.1128/JB.00538-17
25. Alkan N, Espeso EA, Prusky D. 2013. Virulence regulation of phytopathogenic fungi by pH. Antioxid Redox Signal 19:1012–1025. https://doi.org/ 10.1089/ars.2012.5062
26. Cyert MS, Philpott CC. 2013. Regulation of cation balance in *Saccharomyces cerevisiae*. Genetics 193:677–713. https://doi.org/10.1534/genetics.112.147207
27. Fernandes TR, Segorbe D, Prusky D, Di Pietro A. 2017. How alkalinization drives fungal pathogenicity. PLoS Pathog 13:e1006621. https://doi.org/10.1371/journal.ppat.1006621
28. Cho D, Villiers F, Kroniewicz L, Lee S, Seo YJ, Hirschi KD, Leonhardt N, Kwak JM. 2012. Vacuolar CAX1 and CAX3 influence auxin transport in guard cells via regulation of apoplastic pH. Plant Physiol 160:1293–1302. https://doi.org/10.1104/pp.112.201442
29. Geilfus C-M. 2017. The pH of the apoplast: dynamic factor with functional impact under stress. Mol Plant 10:1371–1386. https://doi.org/10.1016/j.molp.2017.09.018
30. Borniego ML, Molina MC, Guiamét JJ, Martinez DE. 2019. Physiological and proteomic changes in the apoplast accompany leaf senescence in *Arabidopsis*. Front Plant Sci 10:1635. https://doi.org/10.3389/fpls.2019.01635
31. Felix G, Regenass M, Boller T. 1993. Specific perception of subnanomolar concentrations of chitin fragments by tomato cells: induction of extracellular alkalinization, changes in protein phosphorylation, and establishment of a refractory state. Plant J 4:307–316. https://doi.org/10.1046/j.1365-313X.1993.04020307.x
32. Felle HH, Waller F, Molitor A, Kogel K-H. 2009. The mycorrhiza fungus *Piriformospora indica* induces fast root-surface pH signaling and primes systemic alkalinization of the leaf apoplast upon powdery mildew infection. Mol Plant Microbe Interact 22:1179–1185. https://doi.org/10.1094/MPMI-22-9-1179
33. Chang X, Nick P. 2012. Defence signalling triggered by Flg22 and Harpin is integrated into a different stilbene output in Vitis cells. PLOS ONE 7:e40446. https://doi.org/10.1371/journal.pone.0040446
34. van Dijk K, Fouts DE, Rehm AH, Hill AR, Collmer A, Alfano JR. 1999. The Avr (effector) proteins HrmA (HopPsyA) and AvrPto are secreted in culture from *Pseudomonas syringae* pathovars via the Hrp (type III) protein secretion system in a temperature- and pH-sensitive manner. J Bacteriol 181:4790–4797. https://doi.org/10.1128/JB.181.16.4790-4797.1999
35. Dawson JE, Seckute J, De S, Schueler SA, Oswald AB, Nicholson LK. 2009. Elucidation of a pH-folding switch in the *Pseudomonas syringae* effector protein AvrPto. Proc Natl Acad Sci U S A 106:8543–8548. https://doi.org/10.1073/pnas.0809138106
36. Do H, Makthal N, VanderWal AR, Saavedra MO, Olsen RJ, Musser JM, Kumaraswami M. 2019. Environmental pH and peptide signaling control virulence of *Streptococcus pyogenes* via a quorum-sensing pathway. Nat Commun 10:2586. https://doi.org/10.1038/s41467-019-10556-8
37. Shetty D, Kenney LJ. 2023. A pH-sensitive switch activates virulence in *Salmonella*. Elife 12:e85690. https://doi.org/10.7554/eLife.85690
38. Samira R, Kimball JA, Samayoa LF, Holland JB, Jamann TM, Brown PJ, Stacey G, Balint-Kurti PJ. 2020. Genome-wide association analysis of the strength of the MAMP-elicited defense response and resistance to target leaf spot in sorghum. Sci Rep 10:20817. https://doi.org/10.1038/s41598-020-77684-w
39. O'Leary BM, Rico A, McCraw S, Fones HN, Preston GM. 2014. The infiltration-centrifugation technique for extraction of apoplastic fluid from plant leaves using *Phaseolus vulgaris* as an example. J Vis Exp:52113. https://doi.org/10.3791/52113
40. Roine E, Wei W, Yuan J, Nurmiaho-Lassila E-L, Kalkkinen N, Romantschuk M, He SY. 1997. Hrp pilus: an hrp-dependent bacterial surface appendage produced by *Pseudomonas syringae* pv. *tomato* DC3000. Proc Natl Acad Sci U S A 94:3459–3464. https://doi.org/10.1073/pnas.94.7.3459
41. Swingle B, Thete D, Moll M, Myers CR, Schneider DJ, Cartinhour S. 2008. Characterization of the PvdS-regulated promoter motif in Pseudomonas syringae pv. tomato DC3000 reveals regulon members and insights regarding PvdS function in other pseudomonads. Mol Microbiol 68:871–889. https://doi.org/10.1111/j.1365-2958.2008.06209.x
42. Markel E, Maciak C, Butcher BG, Myers CR, Stodghill P, Bao Z, Cartinhour S, Swingle B. 2011. An extracytoplasmic function sigma factor-mediated cell surface signaling system in *Pseudomonas syringae* pv. tomato DC3000 regulates gene expression in response to heterologous siderophores. J Bacteriol 193:5775–5783. https://doi.org/10.1128/JB.05114-11
43. Markel E, Butcher BG, Myers CR, Stodghill P, Cartinhour S, Swingle B. 2013. Regulons of three *Pseudomonas syringae* pv. tomato DC3000 iron starvation sigma factors. Appl Environ Microbiol 79:725–727. https://doi.org/10.1128/AEM.02801-12

44. Llamas MA, Imperi F, Visca P, Lamont IL. 2014. Cell-surface signaling in *Pseudomonas*: stress responses, iron transport, and pathogenicity. FEMS Microbiol Rev 38:569–597. https://doi.org/10.1111/1574-6976.12078
45. Wang H, Yang Z, Swingle B, Kvitko BH. 2021. AlgU, a conserved sigma factor regulating abiotic stress tolerance and promoting virulence in *Pseudomonas syringae*. MPMI 34:326–336. https://doi.org/10.1094/ MPMI-09-20-0254-CR
46. Damron FH, Yu HD. 2011. *Pseudomonas aeruginosa* MucD regulates the alginate pathway through activation of MucA degradation via MucP proteolytic activity. J Bacteriol 193:286–291. https://doi.org/10.1128/JB.01132-10
47. Schurr MJ, Martin DW, Mudd MH, Hibler NS, Boucher JC, Deretic V. 1993. The algD promoter: regulation of alginate production by *Pseudomonas aeruginosa* in cystic fibrosis. Cell Mol Biol Res 39:371–376.
48. Baynham PJ, Brown AL, Hall LL, Wozniak DJ. 1999. Pseudomonas aeruginosa AlgZ, a ribbon-helix-helix DNA-binding protein, is essential for

alginate synthesis and algD transcriptional activation. Mol Microbiol 33:1069–1080. https://doi.org/10.1046/j.1365-2958.1999.01550.x 49. Ferreiro M-D, Nogales J, Farias GA, Olmedilla A, Sanjuán J, Gallegos MT. 2018. Multiple CsrA proteins control key virulence traits in *Pseudomonas syringae* pv. tomato DC3000. Mol Plant Microbe Interact 31:525–536. https://doi.org/10.1094/MPMI-09-17-0232-R
50. Shao X, Tan M, Xie Y, Yao C, Wang T, Huang H, Zhang Y, Ding Y, Liu J, Han L, Hua C, Wang X, Deng X. 2021. Integrated regulatory network in *Pseudomonas syringae* reveals dynamics of virulence. Cell Rep 34:108920. https://doi.org/10.1016/j.celrep.2021.108920
51. Chatterjee A, Cui Y, Yang H, Collmer A, Alfano JR, Chatterjee AK. 2003. GacA, the response regulator of a two-component system, acts as a master regulator in *Pseudomonas syringae* pv. tomato DC3000 by controlling regulatory RNA, transcriptional activators, and alternate sigma factors. Mol Plant Microbe Interact 16:1106–1117. https://doi.org/10.1094/MPMI.2003.16.12.1106
52. Deng X, Lan L, Xiao Y, Kennelly M, Zhou J-M, Tang X. 2010. *Pseudomonas syringae* two-component response regulator RhpR regulates promoters carrying an inverted repeat element. Mol Plant Microbe Interact 23:927–939. https://doi.org/10.1094/MPMI-23-7-0927
53. Martínez-Granero F, Navazo A, Barahona E, Redondo-Nieto M, Rivilla R, Martín M. 2012. The Gac-Rsm and SadB signal transduction pathways converge on AlgU to downregulate motility in *Pseudomonas fluorescens*. PLoS ONE 7:e31765. https://doi.org/10.1371/journal.pone.0031765
54. Taguchi F, Ichinose Y. 2013. Virulence factor regulator (Vfr) controls virulence- associated phenotypes in *Pseudomonas syringae* pv. *tabaci* 6605 by a quorum sensing- independent mechanism. Mol Plant Pathol 14:279–292. https://doi.org/10.1111/mpp.12003
55. O'Malley MR, Chien C-F, Peck SC, Lin N-C, Anderson JC. 2020. A revised model for the role of GacS/GacA in regulating type III secretion by *Pseudomonas syringae* pv. *tomato* DC3000. Mol Plant Pathol 21:139–144. https://doi.org/10.1111/mpp.12876
56. Crabill E, Joe A, Block A, van Rooyen JM, Alfano JR. 2010. Plant immunity directly or indirectly restricts the injection of type III effectors by the *Pseudomonas syringae* type III secretion system. Plant Physiol 154:233–244. https://doi.org/10.1104/pp.110.159723
57. Liu Y, Zhang H, Wang J, Gao W, Sun X, Xiong Q, Shu X, Miao Y, Shen Q, Xun W, Zhang R. 2024. Nonpathogenic *Pseudomonas syringae* derivatives and its metabolites trigger the plant "cry for help" response to assemble disease suppressing and growth promoting rhizomicrobiome. Nat Commun 15:1907. https://doi.org/10.1038/s41467-024-46254-3
58. Lovelace AH, Smith A, Kvitko BH. 2018. Pattern-triggered immunity alters the transcriptional regulation of virulence-associated genes and induces the sulfur starvation response in *Pseudomonas syringae* pv. *tomato* DC3000. Mol Plant Microbe Interact 31:750–765. https://doi.org/10.1094/MPMI-01-18-0008-R
59. Wang H, Smith A, Lovelace A, Kvitko BH. 2022. In planta transcriptomics reveals conflicts between pattern-triggered immunity and the AlgU sigma factor regulon. PLoS ONE 17:e0274009. https://doi.org/10.1371/journal.pone.0274009
60. Yu X, Lund SP, Greenwald JW, Records AH, Scott RA, Nettleton D, Lindow SE, Gross DC, Beattie GA. 2014. Transcriptional analysis of the global regulatory networks active in *Pseudomonas syringae* during leaf colonization. MBio 5:e01683-14. https://doi.org/10.1128/mBio.01683-14
61. Wood LF, Leech AJ, Ohman DE. 2006. Cell wall-inhibitory antibiotics activate the alginate biosynthesis operon in *Pseudomonas aeruginosa*: roles of sigma (AlgT) and the AlgW and Prc proteases. Mol Microbiol 62:412–426. https://doi.org/10.1111/j.1365-2958.2006.05390.x
62. Cezairliyan BO, Sauer RT. 2009. Control of *Pseudomonas aeruginosa* AlgW protease cleavage of MucA by peptide signals and MucB. Mol Microbiol 72:368–379. https://doi.org/10.1111/j.1365-2958.2009.06654.x
63. Schreiber KJ, Desveaux D. 2011. AlgW regulates multiple *Pseudomonas syringae* virulence strategies. Mol Microbiol 80:364–377. https://doi.org/10.1111/j.1365-2958.2011.07571.x
64. Li T, Song Y, Luo L, Zhao N, He L, Kang M, Li C, Zhu Y, Shen Y, Zhao C, Yang J, Huang Q, Mou X, Zong Z, Yang J, Tang H, He Y, Bao R. 2021. Molecular basis of the versatile regulatory mechanism of HtrA-type protease AlgW from *Pseudomonas aeruginosa*. MBio 12:e03299-20. https://doi.org/10.1128/mBio.03299-20
65. Muller C, Bang I-S, Velayudhan J, Karlinsey J, Papenfort K, Vogel J, Fang FC. 2009. Acid stress activation of the σE stress response in *Salmonella enterica* serovar Typhimurium. Mol Microbiol 71:1228–1238. https://doi.org/10.1111/j.1365-2958.2009.06597.x
66. Rahme LG, Mindrinos MN, Panopoulos NJ. 1992. Plant and environmental sensory signals control the expression of hrp genes in *Pseudomonas syringae* pv. phaseolicola. J Bacteriol 174:3499–3507. https://doi.org/10.1128/jb.174.11.3499-3507.1992
67. Xiao Y, Lu Y, Heu S, Hutcheson SW. 1992. Organization and environmental regulation of the Pseudomonas syringae pv. syringae 61 hrp cluster. J Bacteriol 174:1734–1741. https://doi.org/10.1128/jb.174.6.1734-1741.1992
68. Marman HE, Mey AR, Payne SM. 2014. Elongation factor P and modifying enzyme PoxA are necessary for virulence of *Shigella flexneri*. Infect Immun 82:3612–3621. https://doi.org/10.1128/IAI.01532-13
69. Bajunaid W, Haidar-Ahmad N, Kottarampatel AH, Ourida Manigat F, Silué N, Tchagang CF, Tomaro K, Campbell-Valois F-X. 2020. The T3SS of *Shigella*: expression, structure, function, and role in vacuole escape. Microorganisms 8:1933. https://doi.org/10.3390/microorganisms8121933
70. Wimmi S, Balinovic A, Jeckel H, Selinger L, Lampaki D, Eisemann E, Meuskens I, Linke D, Drescher K, Endesfelder U, Diepold A. 2021. Dynamic relocalization of cytosolic type III secretion system components prevents premature protein secretion at low external pH. Nat Commun 12:1625. https://doi.org/10.1038/s41467-021-21863-4
71. Rappl C, Deiwick J, Hensel M. 2003. Acidic pH is required for the functional assembly of the type III secretion system encoded by *Salmonella* pathogenicity island 2. FEMS Microbiol Lett 226:363–372. https://doi.org/10.1016/S0378-1097(03)00638-4
72. Yu X-J, McGourty K, Liu M, Unsworth KE, Holden DW. 2010. pH sensing by intracellular *Salmonella* induces effector translocation. Science 328:1040–1043. https://doi.org/10.1126/science.1189000
73. Expert D, Enard C, Masclaux C. 1996. The role of iron in plant hostpathogen interactions. Trends Microbiol 4:232–237. https://doi.org/10.1016/0966-842X(96)10038-X
74. Soares MP, Weiss G. 2015. The Iron age of host-microbe interactions. EMBO Rep 16:1482–1500. https://doi.org/10.15252/embr.201540558
75. Weinberg ED. 1975. Nutritional immunity. Host's attempt to withold iron from microbial invaders. JAMA 231:39–41. https://doi.org/10.1001/jama.231.1.39
76. Spaan AN, Reyes-Robles T, Badiou C, Cochet S, Boguslawski KM, Yoong P, Day CJ, de Haas CJC, van Kessel KPM, Vandenesch F, Jennings MP, Le Van Kim C, Colin Y, van Strijp JAG, Henry T, Torres VJ. 2015. *Staphylococcus aureus* targets the Duffy antigen receptor for chemokines (DARC) to lyse erythrocytes. Cell Host Microbe 18:363–370. https://doi.org/10.1016/j.chom.2015.08.001
77. Anderson JC, Wan Y, Kim Y-M, Pasa-Tolic L, Metz TO, Peck SC. 2014. Decreased abundance of type III secretion system-inducing signals in Arabidopsis mkp1 enhances resistance against *Pseudomonas syringae*. Proc Natl Acad Sci U S A 111:6846–6851. https://doi.org/10.1073/pnas.1403248111
78. King EO, Ward MK, RANEY DE. 1954. Two simple media for the demonstration of pyocyanin and fluorescin. J Lab Clin Med 44:301–307.
79. Bertani G. 1951. Studies on lysogenesis. I. The mode of phage liberation by lysogenic *Escherichia coli*. J Bacteriol 62:293–300. https://doi.org/10.1128/jb.62.3.293-300.1951
80. Choi K-H, Kumar A, Schweizer HP. 2006. A 10-min method for preparation of highly electrocompetent *Pseudomonas aeruginosa* cells: application for DNA fragment transfer between chromosomes and plasmid transformation. J Microbiol Methods 64:391–397. https://doi.org/10.1016/j.mimet.2005.06.001
81. Mijatović J, Severns PM, Kemerait RC, Walcott RR, Kvitko BH. 2021. Patterns of seed-to-seedling transmission of *Xanthomonas citri* pv. *malvacearum*, the causal agent of cotton bacterial blight. Phytopathology 111:2176–2184. https://doi.org/10.1094/PHYTO-02-21-0057-R
82. Kvitko BH, Collmer A. 2011. Construction of *Pseudomonas syringae* pv. tomato DC3000 mutant and polymutant strains. Methods Mol Biol 712:109–128. https://doi.org/10.1007/978-1-61737-998-7_10

83. Ferreira AO, Myers CR, Gordon JS, Martin GB, Vencato M, Collmer A, Wehling MD, Alfano JR, Moreno-Hagelsieb G, Lamboy WF, DeClerck G, Schneider DJ, Cartinhour SW. 2006. Whole-genome expression profiling defines the HrpL regulon of *Pseudomonas syringae* pv. tomato DC3000, allows de novo reconstruction of the Hrp cis clement, and identifies novel coregulated genes. Mol Plant Microbe Interact 19:1167–1179. https://doi.org/10.1094/MPMI-19-1167
84. Smith A, Lovelace AH, Kvitko BH. 2018. Validation of RT-qPCR approaches to monitor *Pseudomonas syringae* gene expression during infection and exposure to pattern-triggered immunity. Mol Plant Microbe Interact 31:410–419. https://doi.org/10.1094/MPMI-11-17-0270TA